

FRB-periodicity: weak pulsar in tight early B-star binary

Maxim Lyutikov, Maxim Barkov, Dimitrios Giannios

Department of Physics, Purdue University, 525 Northwestern Avenue, West Lafayette, IN
47907-2036

ABSTRACT

The 16 days periodicity observed in FRB 180916.J0158+65 by the CHIME telescope is consistent with a tight, stellar mass binary system of semi-major axis $\sim 10^{12}$ cm. The primary is an early B-type star with mass loss rate $\dot{M} \sim 10^{-8} - 10^{-10} M_{\odot} \text{ yr}^{-1}$. The observed periodicity is not intrinsic to the FRBs' source, but is due to the orbital phase-dependent modulation of the absorption conditions in the B-star's wind. Relatively narrow activity window implies that the companion's wind dynamically dominates the pulsar wind, $\eta = L_{sd}/(\dot{M}v_w c) \leq 1$, where L_{sd} is pulsar spin-down, \dot{M} is companion's wind mass loss rate and v_w is its velocity. More massive O stars produce denser wind that are optically thick to radii much large than the the orbital separation. Condition $\eta \leq 1$ requires mildly powerful pulsar with $L_{sd} \sim 10^{34} - 10^{36} \text{ erg s}^{-1}$. The observations are consistent with magnetically-powered radio emission originating in the magnetospheres of strongly magnetized neutron stars, the classical magnetars.

1. FRB periodicity due to the orbital motion with B-star companion

CHIME collaboration announced $P = 16$ days periodicity observed in FRB 180916.J0158+65 (The CHIME/FRB Collaboration et al. 2020). This is an important set of observations which sheds light on the origin of FRBs, as we discuss in the present Letter.

Let's first assume that the observed periodicity is due to orbital motion. The orbital semi-major axis then evaluates to

$$P = 2\pi \sqrt{\frac{a^3}{GM_{\odot}(m_{PSR} + m_{MS})}}$$

$$a = 1.8 \times 10^{12} \text{ cm} (m_{MS} + m_{PSR})^{1/3} \quad (1)$$

where m_{PSR} is (the presumed) neutron star's mass and m_{MS} is the companion's mass (presumed to be a Main Sequence star) in Solar masses.

Both the pulsar, the *loci* of the FRB, and the companion produce winds: relativistic wind by the pulsar and wind with velocity $v_w \sim \text{few } 10^3 \text{ km s}^{-1}$ by the star (Vink et al. 2001). We hypothesize that the observed periodicity is due to absorption of the FRB pulses in the companion’s wind, see Fig. 1.

The interacting pulsar’s and the primaries’ winds (primary is likely to be a massive main sequence star) create a conically shaped cavity around the less powerful source. The primaries’ winds can be highly optically thick at radio waves to free-free absorption, while the relativistic pulsar wind is, basically, transparent to radio waves. A transparent cone-like zone is created behind the pulsar, modified into spiral structure by the orbital motion.

The radio waves propagating within the wind do not experience free-free absorption. After they re-enter the B’stars wind, at larger radii, the winds density, and the corresponding absorption coefficient, are substantially reduced. Thus, the dynamics of interacting winds creates transparency windows behind a pulsar (Bosch-Ramon & Barkov 2011; Bosch-Ramon et al. 2012, 2015).

Since the active window is less than 50 % of the orbital period, *the companion’s wind should dominate over the pulsar’s wind*. This requires that the momentum parameter η is less than unity,

$$\eta = \frac{L_{sd}}{\dot{M}v_w c} \leq 1 \quad (2)$$

In addition, the typical opening of the transparency wedge behind a pulsar seen in simulations of Bosch-Ramon et al. (2015) is $\sim 15 - 20^\circ$; this is mostly independent of the momentum parameter η . This is consistent with the active phase observed in FRB 180916.J0158+65.

If at the location of the pulsar the wind is still mildly, $\tau \leq 10^3$, optically thick to infinity, and the observer’s line of sight passes close to equatorial plan, within $\sim 15 - 20^\circ$, the cavity created by the pulsar’s wind can reduce the absorption optical depth (by as much as a factor of 10^3). In addition, the density of the wind will be largest in the head part of the bow shock, both due to shock compression (by a fact of 4, hence the free-free absorption coefficient is larger by a factor of 16).

2. The model

Simulations of Bosch-Ramon et al. (2015), see also Fig. 1, demonstrate that the wind cavity can extend 10-20 times the star separation radius. In the estimates below we parametrize the location of the “back wall of the cavity” as $\eta_a a$, and normalize the numerical

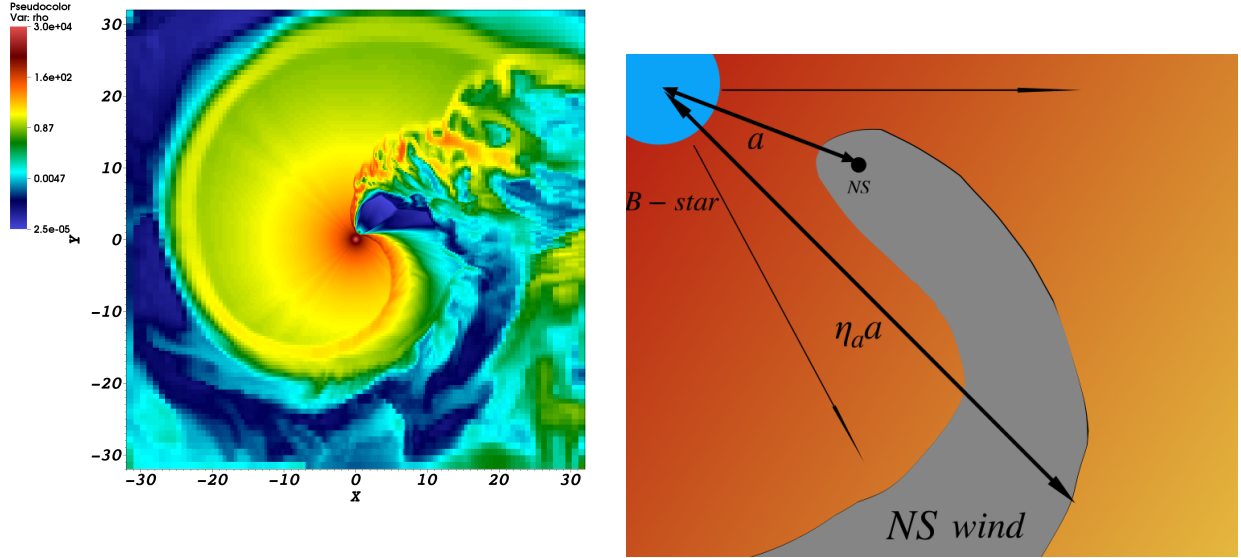


Fig. 1.— Left panel: reprocessed simulations of Bosch-Ramon et al. (2015) of interacting winds of B-star and pulsar’s. Right panel: artistic image of the interacting winds. The pulsar wind creates a narrow low density cavity that extends to distances much larger than the orbital separation by a factor $\eta_a \sim 10 - 20$. At that point the density is lower by η_a^2 , the absorption coefficient is reduced by η_a^4 , and optically depth by η_a^3 .

estimates to $\eta_a = 10\eta a, 10$

The free-free optical depth from the location of “back wall of the cavity” to infinity should be of the order of unity for radio waves to escape. Using the free-free-absorption coefficient κ_{ff} (Lang 1999), assuming temperature $T = 10^4$ K, and scaling the ” “back wall” radius with (1), we find

$$\begin{aligned} \kappa_{ff} &= 3.28 \times 10^{-7} T_4^{-1.35} \nu_{1GHz}^{-2.1} n^2 \frac{a}{pc} \\ \dot{M} &= 4\pi n m_p (\eta_a a)^2 v_w n \\ \tau_{ff} &\sim 1 \times \eta_a^{-3} \dot{M}_{-10}^2 \nu_{1GHz}^{-2.1} = 10^{-3} \times \eta_{a,10}^{-3} \dot{M}_{-10}^2 \nu_{1GHz}^{-2.1} \end{aligned} \quad (3)$$

So, a mass loss rate of $\dot{M} = 10^{-10} M_\odot/yr$ can give substantial optical depth to free-free absorption if the “back wall of the cavity” extends only to $\sim a$. For larger extents, the optical depth drops precipitously, as η_a^{-3} , allowing for larger $\dot{M} \sim \text{few} \times 10^{-8} M_\odot \text{ yr}^{-1}$.

Using mass loss rate \dot{M} from (3) and requiring of companion’s momentum dominance

in the wind-wind interaction, we estimate

$$L_{sd} \leq 2 \times 10^{34} \eta_a^{3/2} \text{ergs}^{-1} M_{\odot, -10} \text{ergs}^{-1} \quad (4)$$

(This evaluates for $L_{sd} \sim 10^{36} \text{ergs}^{-1}$ for $\eta_a = 10$.) Thus, the pulsar should produce mildly strong winds with power $\sim 10^{34} - 10^{36} \text{ergs}^{-1}$ depending on the strength of the companion's wind.

In contrast, for powerful Crab-like pulsar the required mass loss rate is

$$\dot{M} \geq 5 \times 10^{-7} M_{\odot} \text{yr}^{-1} L_{sd, 38}, v_{w, 3}^{-1} \quad (5)$$

Such wind, achievable in early O-type stars, will have very large optical depths, both at the location of the pulsar, and of the “back wall”.

$$\tau_{ff} = 10^5 \eta_a^{-3} m_{MS}^{-1} M_{\odot, -7}^2 \nu_{1 \text{GHz}}^{-2.1} \quad (6)$$

The model limits the mass loss rate from below (the wind-wind interaction should be dominated by the Main Sequence star), and from above (too powerful winds are optically thick to free-free absorption way to too large distances). Early B-type stars, \sim B0-B5, fit the required mass loss range. They have highly different mass loss rates, from 10^{-9} for the hottest B0 stars, to 10^{-12} for cooler later types (Vink et al. 2001; Krtička 2014). In addition, the radius of a B0 star approaches $10R_{\odot} = 7 \times 10^{11} \text{cm}$, of the order of the orbital separation. This also implies that the companion cannot be an O-star - those are too big for the inferred orbit. We infer that the primary should early type, B0-B5, star.

3. Unlikely alternative: FRB variations due to geodetic precession

Another possible source of variability is a the geodetic precession that make the active region periodically aligned with the line of sight. For example, in the binary pulsar PSR 0737 the geodetic precession lead to the disappearance of the PSR 0737B (Breton et al. 2008; Lomiashvili & Lyutikov 2014). To have a geodetic precession of only 16 days the required orbital size is

$$\Omega_G = \left(\frac{2\pi}{P} \right)^{5/3} \left(\frac{GM_{\odot}}{c^3} \right)^{5/3} \left(\frac{m_{MS}(4m_{PSR} + 3m_{MS})}{2(m_{PSR} + m_{MS})^{4/3}} \right)$$

$$a = 2 \times 10^9 \text{cm} \frac{(m_{MS}(4m_{PSR} + 3m_{MS}))^{2/5}}{(m_{PSR} + m_{MS})^{1/5}} \quad (7)$$

Gravitational decay time is still sufficiently long,

$$t_{GW} = 670 \text{yr} \frac{m_{MS}^{2/5}}{m_{PSR}} \quad (8)$$

(where $m_{MS} \geq m_{PSR}$ was assumed).

The system with separation of (7) will be exceptional. Strong modifications of the magnetospheric properties may be expected in this case. For example, setting separation equal to the light cylinder, the period would be 0.75 seconds. Strong wind-magnetosphere interactions are expected, similar to the case of the binary pulsar PSR0737A/B Lyutikov (2004); Lyutikov & Thompson (2005); Lomiashvili & Lyutikov (2014). Note, though, that PSR0737B is/was an *exceptionally weak pulsar* - it cannot not be used as an model for FRBs, the most powerful radio emitters.

Can still the radio emission be induced in FRB 180916.J0158+65 by the interactions of the companions? The orbital motionally-induced electric potential potential and luminosity for scaling (7) estimate to

$$\begin{aligned}\Phi_{orb} &= eBa\beta_{orb} = 2 \times 10^{13} b_q \text{ eV} \\ L_{orb} &\sim (\Phi_{orb}/e)^2 c = 2 \times 10^{31} b_q^2 \text{ ergs}^{-1}\end{aligned}\quad (9)$$

where we scaled the surface magnetic field to quantum field, $b_q = B_{NS}/B_Q$, $B_Q = m_e^2 c^3 / (3\hbar)$.

Estimates (9) give very weak power, even for quantum-strong magnetic fields, and small potential. We conclude that even in the tightest orbit case of geodetically induced precession, the powers expected due to the interaction of the binaries are very small. *Hence we conclude that binarity is not a cause of FRB emission.*

4. Predictions

Next we discuss the predictions of the model. As a simple educated guess, we predict variations of the dispersion measure within the observed window, and increase of the of activity window at higher frequencies. First we give simple order-of-magnitude estimates, and then demonstrate that the reality is likely be more complicated.

DM variations. In a homogeneous wind a DM from a given point located distance a from the central star and propagating with angle ϕ with respect to the radial direction, is

$$DM(\phi) = \int_a^\infty \frac{n_0 a^2}{x^2 + (x-a)^2 \tan^2 \phi} \frac{dx}{\cos \phi} = \frac{\phi}{\sin \phi} DM_0 \quad (10)$$

where

$$DM_0 = DM(\phi = 0) = \int_a^\infty \frac{n_0 a^2}{x^2} dx \approx 1.06 \dot{M}_{-10} \quad (11)$$

the dispersion measure for a radial ray. (For larger ϕ the DM and the optical depth, see below, increase wot *theta* as the light ray passes longer distance at higher densities). This is

the upper limit on the DM variations. Since the “back of the wall” is located at $\eta_a \sim 10$, the expected DM variations are $\sim 10^{-2}$. This is consistent with observations (The CHIME/FRB Collaboration et al. 2020).

Optical depth variations Similarly, in a homogeneous wind an optical depth to a given point (assuming isothermal wind) is

$$\begin{aligned}\tau(\phi) &\propto \int_a^\infty \left(\frac{n_0 a^2}{x^2 + (x-a)^2 \tan^2 \phi} \right)^2 \frac{dx}{\cos \phi} \\ \tau(\phi) &= \frac{3}{2} (\phi \csc^3(\phi) - \cot(\phi) \csc(\phi)) \tau_0\end{aligned}\quad (12)$$

where $\tau_0 = \tau(\phi = 0)$. The optical depth for radial propagation depends on frequency, Eq. 3

$$\tau_0 \propto \nu^{-2.1} \quad (13)$$

Let ν_0 be the frequency such that $\tau_0(\nu_0 = 1)$. At higher frequencies optical depth of 1 is reached at, Fig. 2

Above estimates assume idealized smooth wind. As numerical simulations demonstrate, Fig. 1, the plasma around the bow shock is highly inhomogeneous. The pulsar wind creates a tail cavity and an accumulation of dense material around the head. These plasma “wall” will have especially large effect on the free-free absorption, since it depends on density squared. A plasma wall can be opaque to a broad range of frequencies, erasing simple correlation between the active window and the observing frequency

Next, we calculated dispersion measure and free-free absorption in the stellar and pulsar interacting winds based on the 3D RHD simulation published in Bosch-Ramon et al. (2015). In figure 3, we present profiles of the integrated density, $\int n \propto DM$ and integrated density squared, $\int n \propto \tau$ (the absorption optical depths) along different lines of sight. Fig. 3 demonstrates that at each moment there is a narrow transparent window with a duration from ~ 0.1 (close to apoastron) to ~ 0.3 (close to periastron) orbital period. Interestingly, a “wide” window can be affected by turbulent motion and can be chaotically transparent and opaque from orbit to orbit.

On the one hand, the DM and free-free absorption have a good correlation, the transparent window corresponds to a minimum of DM and it can explain the small change of DM for repeating FRBs. On the other hand, the variations of the DM with the transparent window are smaller by a factor of few than the overall variations.

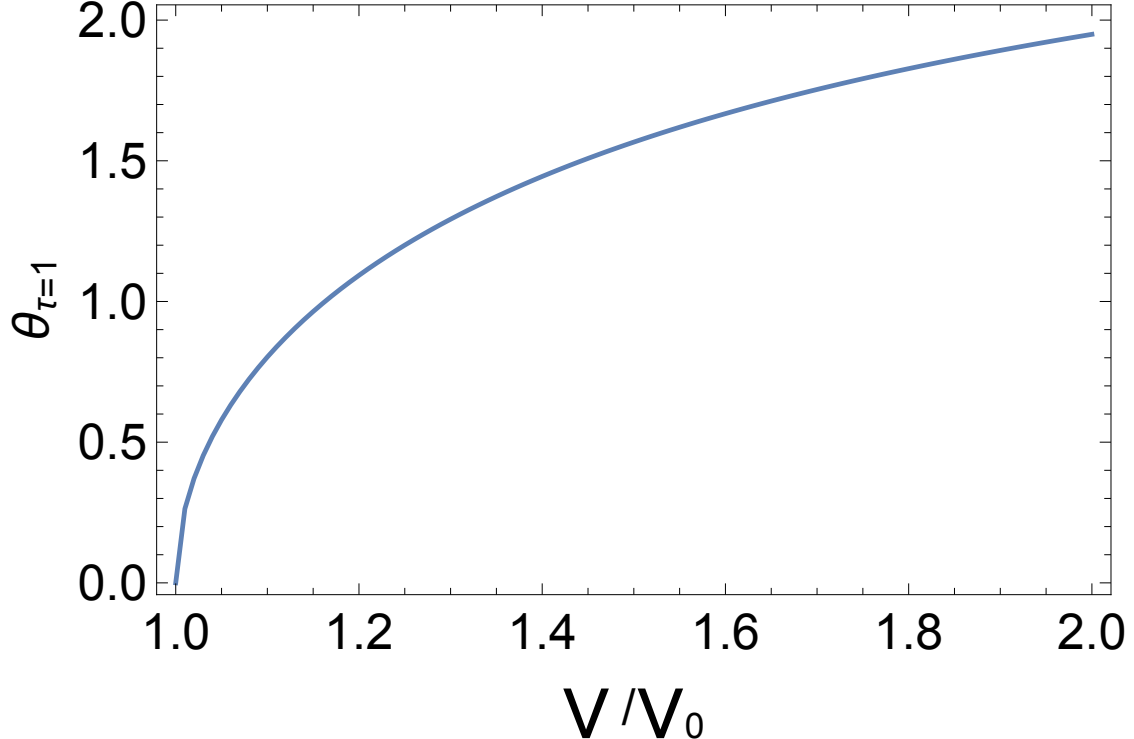


Fig. 2.— Dependence of the transparency angle ϕ on the observing frequency ν/ν_0 in idealized homogeneous wind. At the base frequency ν_0 the radial (outward propagating) rays have $\tau = 1$. At larger frequencies the rays at larger angles can escape, see also Fig. 3

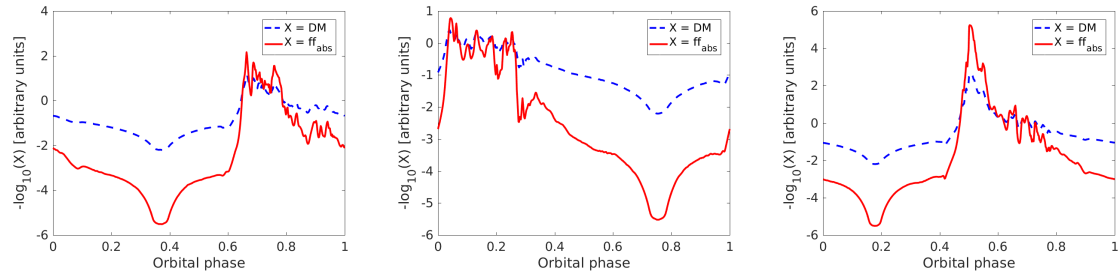


Fig. 3.— Profiles of the DM (dashed blue) and absorption optical depth (solid red) along different lines of sight calculated at three different orbital phases (close to apoastron - left, intermediate phase - center and close to periastron - right). Large values of $-\log \tau$ (red curves) correspond to transparency window.

5. Discussion

In this Letter we discuss a model of periodicity observed in FRB 180916.J0158+65 by CHIME telescope (The CHIME/FRB Collaboration et al. 2020). The working model is that the FRBs are produced with neutron star’s that orbits a B-star primary. The periodicity arises due to free-free absorption in the primary’s (of the B-star’s) wind. Thus, we argue that the observed periodicity is a property of a particular system and is likely not essential for the FRB production. On the other hand, the association of an FRB with a compact stellar binary further strengthens the magnetospheric *loci* of FRBs, as argued by Lyutikov et al. (2016); Lyutikov (2019a,b) (see reviews by Cordes & Chatterjee 2019; Petroff et al. 2019). Note that FRB 180916.J0158+65 also shows narrow emission bands drifting down in frequency - this is naturally interpreted as plasma laser operating in neutron star’s magnetosphere and showing radius-to-frequency mapping (Lyutikov 2019b).

We constrain the companion to be early-type B star: earlier types have too powerful winds that remain heavily optically thick at the inferred orbital separation, while later types produce winds that are too weak - this runs contrary our interpretations of the small orbital activity window as a pointing to momentum dominance of the companion’s wind over the pulsar’s. The companion’s momentum loss should over-power the pulsar’s wind - the pulsar should be weak, with spin-down luminosity $L_{sd} \sim 10^{34} = 10^{36}$ erg s⁻¹. This matches, at the lower end, the spin-down power of the Galactic magnetars.

Periodic transparency can be also achieved by having a highly eccentric orbit - then at an apoastron the radio pulses would sample lower density plasma. We disfavor this possibility since, first, it it predict large active window (since the binary would spend more time at large separations), and secondly, at 16 days the orbit is likely circularized.

Identification of FRBs with neutron stars leaves two possibilities for the energy source: rotational (akin to Crab’s giant pulses Popov et al. 2006; Lyutikov 2007; Mickaliger et al. 2012; Lyutikov et al. 2016), or magnetar-like magnetically powered emission (Lyutikov 2002; Eichler et al. 2002).

To be clear, the term “magnetar” is used in two astrophysically separate settings: (i) powerful X-ray emitters, SRGs and AXPs, (eg Thompson & Duncan 1995; Thompson et al. 2002; Kaspi & Beloborodov 2017) ; (ii) fast pulsar with high magnetic field and high wind power (Usov 1992; Lyutikov 2006; Metzger et al. 2008). In the first case the radiative energy comes from the energy of the magnetic field in the latter case it is the rotational energy (strong magnetic field just serves to quickly transform the rotational energy into the wind. Many models of FRBs employ the second scenario, using the word “magnetar” to mean central source producing rotationally-powered winds (Margalit et al. 2019; Metzger et al.

2019; Beloborodov 2017). We argue that the present observations are inconsistent with the rotationally powered “fast pulsar with high magnetic field”-magnetar concept, but are consistent with magnetically-powered magnetospheric magnetar sources.

The present model has a number of similarities to binary systems containing pulsars. First, binary pulsars PSR 1957 + 20 and PSR 1744 - 24A shows periodic orbital-dependent eclipses (limited to $\sim 10\%$ in phase in case of PSR 1957 + 20 and $\sim 50\%$ in case of PSR 1744 - 24A Lyne et al. 1990; Rasio et al. 1989, 1991). These are mass binary, ablated by the NS’s wind (Phinney et al. 1988), so the wind-wind interaction is dominated by the pulsar’s wind, $\eta \geq 1$. In that case a number of plasma effects, like variations of the DM and pulse delays, do show during the eclipse.

Then, there is a number of γ -ray binaries that contain (or thought to contain) neutron stars (Dubus 2013; Bosch-Ramon et al. 2017; Barkov & Bosch-Ramon 2018)

Overall, the observed periodicity in FRB 180916.J0158+65 does fit with a general concept of neutron stars’ magnetospheres being the *loci* of FRBs. It also confirms that FRBs are not rotationally powered (since the present model requires that the pulsar wind should mild/weak). The magnetically powered model, radio emission generated in the magnetospheres of neutron stars remains the most probably in our view.

ML would like to acknowledge support by NASA grant 80NSSC17K0757 and NSF grants 10001562 and 10001521. We would like to thank Victoria Kaspi for discussions and Yegor Lyutikov for help with the illustration.

REFERENCES

Barkov, M. V., & Bosch-Ramon, V. 2018, MNRAS, 479, 1320

Beloborodov, A. M. 2017, ApJ, 843, L26

Bosch-Ramon, V., & Barkov, M. V. 2011, A&A, 535, A20

Bosch-Ramon, V., Barkov, M. V., Khangulyan, D., & Perucho, M. 2012, A&A, 544, A59

Bosch-Ramon, V., Barkov, M. V., Mignone, A., & Bordas, P. 2017, MNRAS, 471, L150

Bosch-Ramon, V., Barkov, M. V., & Perucho, M. 2015, A&A, 577, A89

Breton, R. P., Kaspi, V. M., Kramer, M., McLaughlin, M. A., Lyutikov, M., Ransom, S. M., Stairs, I. H., Ferdman, R. D., Camilo, F., & Possenti, A. 2008, Science, 321, 104

Cordes, J. M., & Chatterjee, S. 2019, *ARA&A*, 57, 417

Dubus, G. 2013, *A&A Rev.*, 21, 64

Eichler, D., Gedalin, M., & Lyubarsky, Y. 2002, *ApJ*, 578, L121

Kaspi, V. M., & Beloborodov, A. M. 2017, *ARA&A*, 55, 261

Krtička, J. 2014, *A&A*, 564, A70

Lang, K. R. 1999, *Astrophysical formulae*

Lomiashvili, D., & Lyutikov, M. 2014, *MNRAS*, 441, 690

Lyne, A. G., Manchester, R. N., D’Amico, N., Staveley-Smith, L., Johnston, S., Lim, J., Fruchter, A. S., Goss, W. M., & Frail, D. 1990, *Nature*, 347, 650

Lyutikov, M. 2002, *ApJ*, 580, L65

—. 2004, *MNRAS*, 353, 1095

—. 2006, *New Journal of Physics*, 8, 119

—. 2007, *ArXiv e-prints*, 705

—. 2019a, *arXiv e-prints*, arXiv:1901.03260

—. 2019b, *arXiv e-prints*, arXiv:1909.10409

Lyutikov, M., Burzawa, L., & Popov, S. B. 2016, *MNRAS*, 462, 941

Lyutikov, M., & Thompson, C. 2005, *ApJ*, 634, 1223

Margalit, B., Berger, E., & Metzger, B. D. 2019, *ApJ*, 886, 110

Metzger, B. D., Margalit, B., & Sironi, L. 2019, *MNRAS*, 485, 4091

Metzger, B. D., Quataert, E., & Thompson, T. A. 2008, *MNRAS*, 385, 1455

Mickaliger, M. B., McLaughlin, M. A., Lorimer, D. R., Langston, G. I., Bilous, A. V., Kondratiev, V. I., Lyutikov, M., Ransom, S. M., & Palliyaguru, N. 2012, *ApJ*, 760, 64

Petroff, E., Hessels, J. W. T., & Lorimer, D. R. 2019, *A&A Rev.*, 27, 4

Phinney, E. S., Evans, C. R., Blandford, R. D., & Kulkarni, S. R. 1988, *Nature*, 333, 832

Popov, M. V., Soglasnov, V. A., Kondrat'Ev, V. I., Kostyuk, S. V., Ilyasov, Y. P., & Oreshko, V. V. 2006, *Astronomy Reports*, 50, 55

Rasio, F. A., Shapiro, S. L., & Teukolsky, S. A. 1989, *ApJ*, 342, 934

—. 1991, *A&A*, 241, L25

The CHIME/FRB Collaboration, Amiri, M., Andersen, B. C., Bandura, K. M., Bhardwaj, M., Boyle, P. J., Brar, C., Chawla, P., Chen, T., Cliche, J. F., Cubranic, D., Deng, M., Denman, N. T., Dobbs, M., Dong, F. Q., Fand ino, M., Fonseca, E., Gaensler, B. M., Giri, U., Good, D. C., Halpern, M., Hessels, J. W. T., Hill, A. S., Höfer, C., Josephy, A., Kania, J. W., Karuppusamy, R., Kaspi, V. M., Keimpema, A., Kirsten, F., Landecker, T. L., Lang, D. A., Leung, C., Li, D. Z., Lin, H. H., Marcote, B., Masui, K. W., Mckinven, R., Mena-Parra, J., Merryfield, M., Michilli, D., Milutinovic, N., Mirhosseini, A., Naidu, A., Newburgh, L. B., Ng, C., Nimmo, K., Paragi, Z., Patel, C., Pen, U. L., Pinsonneault-Marotte, T., Pleunis, Z., Rafiei-Ravandi, M., Rahman, M., Ransom, S. M., Renard, A., Sanghavi, P., Scholz, P., Shaw, J. R., Shin, K., Siegel, S. R., Singh, S., Smegal, R. J., Smith, K. M., Stairs, I. H., Tendulkar, S. P., Tretyakov, I., Vanderlinde, K., Wang, H., Wang, X., Wulf, D., Yadav, P., & Zwaniga, A. V. 2020, arXiv e-prints, arXiv:2001.10275

Thompson, C., & Duncan, R. C. 1995, *MNRAS*, 275, 255

Thompson, C., Lyutikov, M., & Kulkarni, S. R. 2002, *ApJ*, 574, 332

Usov, V. V. 1992, *Nature*, 357, 472

Vink, J. S., de Koter, A., & Lamers, H. J. G. L. M. 2001, *A&A*, 369, 574